The Structure and Variability of Extended S II 1256Å Emission Near Io

R. Carey Woodward, Jr.,[1,6] Fred Roesler,[1,6] Ronald Oliversen,[2,6] William Smyth,[3] H. Warren Moos,[4] Fran Bagenal[5]

Introduction

Since the first Space Telescope Imaging Spectrograph (STIS) observations of Io in 1997 [*Roesler et al.*, 1999], 32 spectrally dispersed STIS images of Io containing the S II 1256Å line have been obtained during eight "visits" or observing sequences (table 1). Each image consists of $2'' \times 25''$ rectangles containing Io, which includes emission out to 15–40 Io radii from the moon, replicated for each emission line present (figure 1). Previous work has concentrated on the neutral S and O emission from Io, primarily on and near Io's disk; here we examine the radial structure of the extended S II 1256Å emission. (In the thirty images studied here, the low dispersion of the G140L grating—0.584Å/pixel—makes it difficult to distinguish between S II 1256Å and possible S I 1251Å emission; the two G140M images, at 0.053Å/pixel, show that no detectable S I 1251Å emission exists.)

Reduction & Analysis

In addition to the problem of overlapping lines common to all spectral features, this analysis is complicated by two factors that collectively are unique to extended ion emission: the presence of background plamsa torus emission, and the existence of an unexpected and poorly-understood "blotch" of dark current in the FUV MAMA detector, which can simulate a broad wings in an emission line.

The "dark glow" in the STIS FUV MAMA detector consists of a uniform dark current, often in excess of the design rate of $\sim 7\times10^{-6}$ counts/sec, and a "blotch" which is peaked in the upper left quadrant of the MAMA. *Landsman* [1998] describes this dark current, presents a "superdark" image consisting of summed dark current from 288 dark images totalling 397,440 seconds of integration, and derives an approximate dependence of global dark rate on the STIS low voltage power supply temperature (LVPST). This LVPST relationship proved to have too much scatter to be useful for our work; we therefore defined a dark function consisting of an adjustable uniform dark current added to the smoothed "superdark" with an adjustable scaling factor, and created a synthetic dark image for each data image by fitting (in the least-square sense) this dark function to the data in the emission-free area of the G140L images between S I 1479Å and S I 1667Å, avoiding Io's neighborhood and the slit image's occulting bar. (Other emission-free areas were used in the G140M images.) This dark function fit the dark areas well and unambiguously, and varied with LVPST in the same manner of (and with the same scatter as) *Landsman* [1998] (figure 2).

We then reduced the images and the synthetic darks using the standard CALSTIS pipeline, removed areas contaminated by other lines, averaged the pixels over $0.1\,R_{Io}$ radial bins in 60° wedges centered on the long slit direction, and finally subtracted the darks from the data (figure 3). We created model slit images using IPTGEM [*Woodward and Smyth*, 1994], calculating each component of the S II 1256Å triplet and convolving them appropriately, and calculated radial profiles from them in the same way. (We did not attempt to deconvolve the data, as this would be difficult and would make little difference outside of $\sim$2–3 R_{Io}.) These model profiles were almost all smaller than the data, so we scaled them to fit the data at $r > 10R_{Io}$, with an adjustable offset.

Results

The results are tabulated in table 1 and plotted in figure 3; the scaling factor is 2–3 in most cases, but could be as high as 6. These scaled models fit the data well outside of $10\,R_{Io}$, but unsurprisingly do not fit the near-Io emission. We believe that a factor of 2–3 is a result of antiquated atomic emission data, but that the rest represents genuine variation in the torus. Of particular interest to us was a large, highly asymmetric brightening in the extended S II 1256Å emission on 14 October 1997, correlated with brightenings in neutral O and S UV lines in the same STIS data and with [O I] 6300Å observed from the ground [*Woodward et al.*, 2000]. This brightening is now seen to be unique in the full dataset, and moreover to be consistent with a > 2-fold brightening of the underlying torus. The near-Io excess emission also increases, but is much more symmetric than was previously believed.

Finally, we chose an image in which the dark current was low and uniform, and the background torus contribution was small and linear (and therefore contributed minimally to the profile shape), subtracted the (scaled) torus model from the data, and compared the the result to the S I 1479Å emission from the same image (figure 4). Contrary to our expectations based on the appearance of the raw data, the two are indistingiushable.

Summary

- Thirty spectrally resolved far-UV images of Io's neighborhood have been studied in the S II 1256Å line. The STIS FUV MAMA "dark glow" proved a significant contaminant in some images; a special reduction technique was developed to mitigate this problem.
- For most images, the 1256Å emission more that $\sim 10\,R_{Io}$ can be characterized by the predicted plasma torus emission, based on Voyager data, with an empirically chosen scaling factor and offset. The scaling factor ranges from 0–6, but is usually 2–3, and is consistent with the variable nature of the plasma torus.
- In particular, the anomalous brightening of this line on 1997/10/14 is consistent with a > 2-fold brightening of the underlying torus. Near-Io emission also jumps, suggesting local S^+ was "lit up" by enhanced torus electron density.
- In at least one image, the 1256Å emission profile not attributable to the "dark glow," a constant background, or the plasma torus, is indistinguishable from the S I 1479Å emission.

Date	Time	Root name	LVPST	ζ	λ_{III}	ϕ_{Io}	TF
10/14/	2:53	O49D01010	36.5	10.6	352.1	241.3	2.4±0.3
1997	3:11	O49D01A10	37.0		0.8	244.0	2.6±0.2
	4:17	O49D01020	38.0		31.2	253.2	2.5±0.1
	4:44	O49D01A20	38.4		43.6	257.0	3.1±0.1
	5:54	O49D01030	39.2		76.0	266.9	4.5±0.1
	6:20	O49D01A30	39.7		88.4	270.7	6.0±0.1
08/23/	17:46	O4XM01030	31.4	5.0	34.2	296.5	1.6±0.5
1998	18:11	O4XM01040	32.3		45.8	300.1	3.7±1.1
	19:25	O4XM01050	34.3		80.0	310.5	0.0±0.6
	19:49	O4XM01060	34.8		90.9	313.8	0.0±1.7
	21:01	O4XM01070	36.3		124.6	324.1	3.1±0.7
	21:24	O4XM01080	36.7		135.1	327.3	6.4±0.6
08/27/	17:23	O4XM02010	40.2	4.2	171.8	27.7	4.2±0.9
1998	18:28	O4XM02020	40.4		202.1	36.9	2.2±0.3
	18:50	O4XM02030	40.6		211.8	39.9	2.9±0.2
	20:08	O4XM02040	40.9		248.3	51.0	2.7±0.2
10/08/	12:16	O5H9A5010	40.9	3.4	77.9	327.9	5.8±1.1
1999	12:36	O5H9A5020	40.9		87.2	330.7	6.1±1.5
10/11/	4:57	O5H906010	37.5	2.9	76.0	156.7	1.1±0.3
1999	5:14	O5H906020	38.0		83.8	159.1	2.3±0.4
	11:24	O5H907010	40.4		255.2	211.5	2.7±3.2
	11:41	O5H907020	40.6		263.0	213.8	1.4±2.4
[M]	12:46	O5H907030	40.6		293.3	223.1	—
[M]	13:07	O5H907040	40.6		302.6	225.9	—
02/20/	9:58	O5H909010	37.5	9.9	60.1	58.7	0.2±0.2
2000	10:15	O5H909020	38.0		67.9	61.1	0.2±0.2
	11:19	O5H909030	38.9		97.6	70.1	2.4±0.3
	11:44	O5H909040	39.2		109.4	73.7	3.3±0.3
02/25/	12:19	O5H9A2010	40.4	9.5	220.2	15.0	2.0±0.5
2000	12:32	O5H9A2020	40.6		226.5	16.9	2.4±0.4
	13:40	O5H9B2010	40.9		257.8	26.5	2.9±0.4
	13:60	O5H9B2020	40.9		267.2	29.3	3.5±0.4

Table 1: *Observational and reduction parameters. Date and time are observation midpoints (UT). LVPST is the STIS Low Voltage Power Supply Temperature (Kelvins).* ζ *is the angle (°) of the line of sight with respect to terrestrial antisunward.* λ_{III} *is Io's System III longitude (°).* ϕ_{Io} *is Io's phase angle; 0° is superior conjunction with Jupiter. TF is the torus model scaling factor that best fits the data. [M] marks G140M (medium spectral resolution) data; others are G140L.*

[1] University of Wisconsin—Madison
[2] NASA/Goddard Space Flight Center
[3] Atmospheric & Environmental Research, Inc.
[4] Johns Hopkins University
[5] University of Colorado
[6] Visiting Astronomer, National Solar Observatory, NOAO

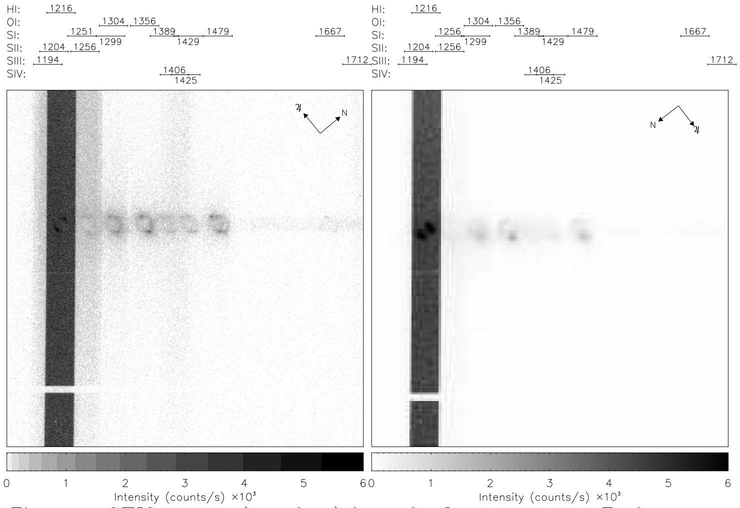

Figure 1: *STIS images (raw data) from the first two visits. Each image is* 1024×1024 *pixels, each* $0.0244''$ *square on the sky plane, with 0.584 Å/pixel dispersion convolved with the spatial information horizontally; thus, for each emission wavelength, a "slit image" appears at a different (but potentially overlapping) position on the detector. Positions of slit images for expected emission wavelengths are shown above the image. The emission of interest in this work is S II 1256Å, next to (and partially overlapping) the bright Lyman-*α *slit image. The small circular features are emission near Io's limb.*

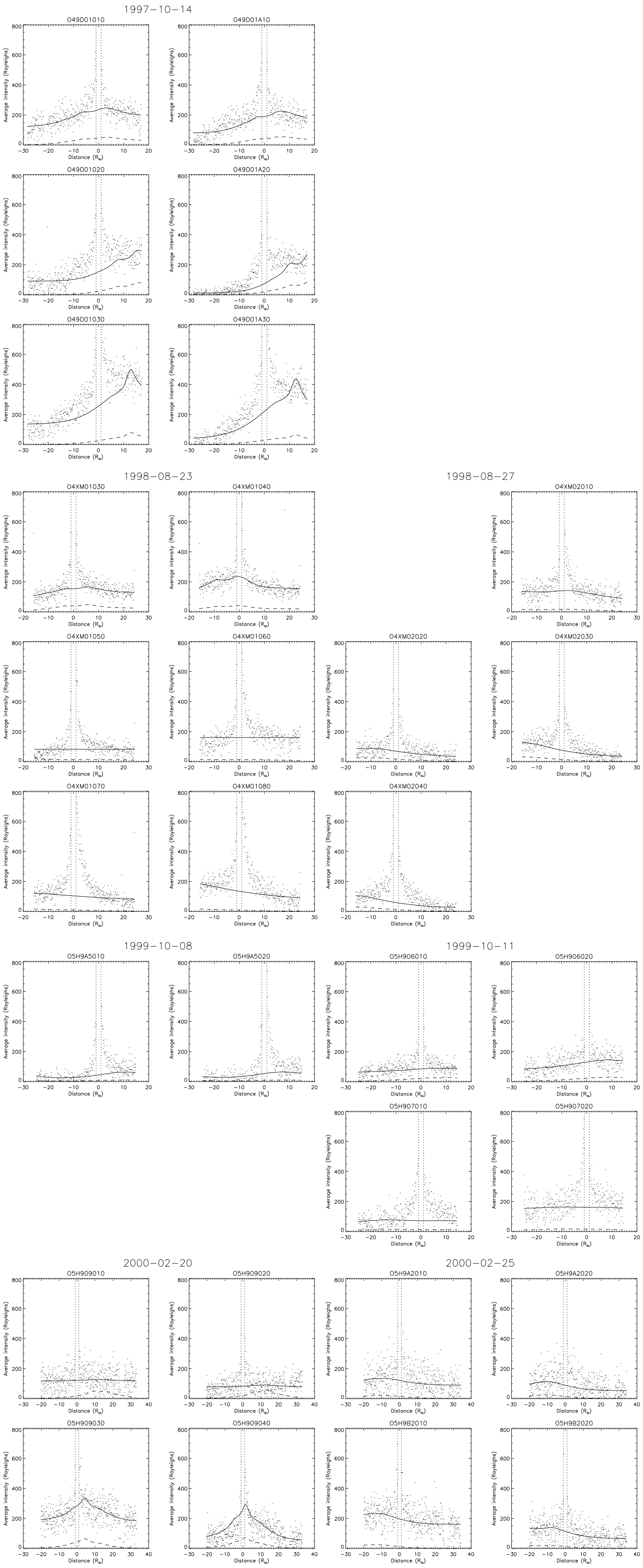

Figure 3: *S II spatial profiles from all G140L data, organized by date or "visit." Each dot is the average of emission in a 0.1* R_{Io} *radial bin in a* 60° *wedge around the long slit direction. Positive abcissa is toward jovian north. The vertical dotted lines mark 1* R_{Io}*; data within these lines are not shown. The dashed lines show the torus emission predicted by a model based on Voyager data [Woodward and Smyth, 1994]; the solid line is the same model emission scaled and offset so as to give the best fit to the emission more than 10* R_{Io} *from Io. (These scaling factors are listed in Table 1.)*

References

Landsman, W., Characteristics of the FUV MAMA Dark Rate, 1998, sTIS IDT report.

Oliversen, R. J., et al., "Sunlit Io Atmospheric [O I] 6300Å Emission and the Plasma Torus", *J. Geophys. Res.*, 2001, in press.

Roesler, F. L., et al., "Far-Ultraviolet Imaging Spectroscopy of Io's Atmosphere with HST/STIS", *Science*, **283**, 353–357, 1999.

Woodward, R. C., Jr., and W. H. Smyth, "Modelling the Io Plasma Torus: Effect of Global Parameters", *Bull. Am. Astron. Soc.*, **26**, 1139, 1994.

Woodward, R. C., Jr., R. J. Oliversen, F. Scherb, and F. L. Roesler, "Synoptic Imaging of the Io Plasma Torus in [S II] 6731Å: Long-term Variability", *Bull. Am. Astron. Soc.*, **32**, 3512, 2000.

Woodward, R. C., Jr., et al., "Simultaneous HST/STIS and Ground-based Observations of Sulfur in the Io Plasma Torus", *Eos*, **81**, S290–S291, 2000.

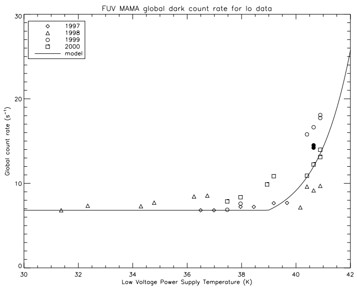

Figure 2: *Measured global dark rate vs. rate computed using STScI algorithm [Landsman, 1998]. Dark circles indicate G140M data; others are G140L. The data are consistent with the model, but unsurprisingly the scatter shows the model to be inadequate for dark current removal.*

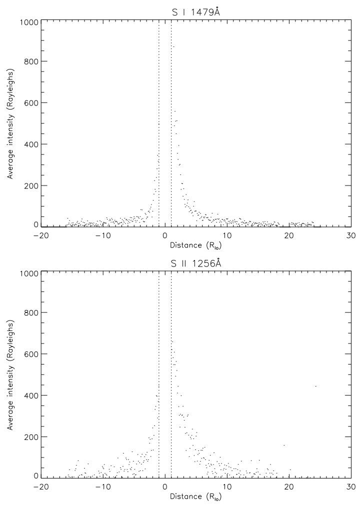

Figure 4: *Comparison of S I 1479Å [upper right] and S II 1256Å [right] emission near Io for image O4XM01070 (chosen for its low dark current and low, linear torus emission). Torus emission has been removed from the latter, which is now indistinguishable from the former.*